MOLECULAR AND CELLULAR BIOLOGY, Mar. 1997, p. 1615–1625 Vol. 17, No. 3
0270-7306/97/$04.00+0

DAP-5, a Novel Homolog of Eukaryotic Translation Initiation Factor 4G Isolated as a Putative Modulator of Gamma Interferon-Induced Programmed Cell Death

NAOMI LEVY-STRUMPF, LOUIS P. DEISS,† HANNA BERISSI, AND ADI KIMCHI*

Department of Molecular Genetics, Weizmann Institute of Science, Rehovot 76100, Israel

Received 7 October 1996/Returned for modification 27 November 1996/Accepted 13 December 1996

A functional approach to gene cloning was applied to HeLa cells in an attempt to isolate cDNA fragments which convey resistance to gamma interferon (IFN-γ)-induced programmed cell death. One of the rescued cDNAs, described in this work, was a fragment of a novel gene, named DAP-5. Analysis of a DAP-5 full-length cDNA clone revealed that it codes for a 97-kDa protein that is highly homologous to eukaryotic translation initiation factor 4G (eIF4G, also known as p220). According to its deduced amino acid sequence, this novel protein lacks the N-terminal region of eIF4G responsible for association with the cap binding protein eIF4E. The N-terminal part of DAP-5 has 39% identity and 63% similarity to the central region of mammalian p220. Its C-terminal part is less homologous to the corresponding region of p220, suggesting that it may possess unique functional properties. The rescued DAP-5 cDNA fragment which conveyed resistance to IFN-γ-induced cell death was expressed from the vector in the sense orientation. Intriguingly, it comprised part of the coding region which corresponds to the less conserved C-terminal part of DAP-5 and directed the synthesis of a 28-kDa miniprotein. The miniprotein exerted a dual effect on HeLa cells. Low levels of expression protected the cells from IFN-γ-induced programmed cell death, while high levels of expression were not compatible with continuous cell growth. The relevance of DAP-5 protein to possible changes in a cell's translational machinery during programmed cell death and growth arrest is discussed.

Functional approaches to gene cloning, based on random inactivation of gene expression, or function, with subsequent growth selection, are very powerful and have proved to be successful in the isolation of growth-suppressive and/or cell death genes. One such approach, called technical knockout, pioneered in our laboratory, was based on random inactivation of genes via the introduction of antisense cDNA expression libraries. Our basic assumption was that a specific inactivation of a critical gene along growth-suppressive pathways would confer some growth advantage to cells that are continuously kept in a growth-restrictive environment. This advantage could then serve as a basis for a forward selection to rescue the relevant cDNA (13).

Interferons (IFNs) were chosen as the specific external triggers, mainly because the types of growth-restrictive scenarios that members of this family exert on cells have been characterized in detail (11, 28, 55). The HeLa–IFN-γ system used for gene rescue is characterized by a biphasic type of response consisting of growth arrest followed by programmed cell death. This biphasic system provided the proper genetic constellation to enable us to determine whether the rescued genes function before or after the pathways of growth arrest and of cell death bifurcate. The introduction of an IFN-responsive DNA element (6) into the vector expressing the cDNA library increased the probability of hitting genes that function downstream of the receptor-generated early signaling events. By this approach, fragments that correspond to five novel genes encoding death-associated proteins (DAPs) and to two known genes, the thioredoxin and cathepsin D protease genes, were isolated (11–13). Other laboratories used similar functional selection strategies, and candidate genes that mediate cell death induced by interleukin-3 deprivation or by T-cell receptor activation were cloned (20, 57).

Transfection of HeLa cells with the antisense cDNA fragments corresponding to either three of the DAP genes (DAP-1 to -3) or cathepsin D protected the transfected cells from IFN-γ-induced cell death with similar time kinetics and to the same extent (11, 12, 30). The full-length sense cDNA corresponding to each of these genes was isolated, antibodies were raised, and the levels of expression, functions, and biochemical properties of the encoded proteins were analyzed. It was found that DAP-1 codes for a basic 15-kDa proline-rich protein, that DAP-2 is a structurally unique 160-kDa calcium/calmodulin-regulated serine/threonine protein kinase (therefore named DAP kinase), and that DAP-3 codes for a 46-kDa protein that carries a potential ATP or GTP binding motif (5, 11, 17, 18, 30). We have also investigated the involvement of cathepsin D protease in programmed cell death and found that this aspartyl protease displays a unique pattern of regulation during cell death and that its proteolytic function is necessary for the execution of apoptosis (12).

In this work, we embarked upon the study of an additional rescued DNA fragment, corresponding to DAP-5, which conferred a phenotype more complex than those of the above-mentioned cDNA clones. We report here that expression of the DAP-5 partial cDNA clone in HeLa cells exerted a dual effect depending on its level of expression. High levels were not compatible with continuous cell growth and eventually resulted in cell death, while low levels protected HeLa cells from cell death. This protective effect provided the basis for the functional cloning of the partial cDNA. Analysis of the corresponding full-length cDNA clone revealed that it codes for a novel 97-kDa protein highly homologous to the eukaryotic translation initiation factor 4G (eIF4G or p220). Comparison of its deduced amino acid sequence with the eIF4G homologs indicated that DAP-5 lacks the N-terminal region of eIF4G, which

* Corresponding author. Phone: 972-8-9342428. Fax: 972-8-9344108.
† Present address: Department of Genetics, University of Illinois at Chicago, Chicago, IL 60612-7309.

TABLE 1. The rescued functional cDNA fragments conferring resistance to IFN-γ

Fragment(s)	Length of cDNA fragment (bp)	Size of endogenous mRNA (kb)	Identity	Orientation in vector	Type of IFN-γ resistance phenotype
230, 254, 255, 258, and 264	320	2.4	DAP-1	Antisense	I
256	367	6.3	DAP-2 (DAP kinase)	Antisense	I
259	252	1.7	DAP-3	Antisense	I
229	370	2.2	Cathepsin D	Antisense	I
241, 248, 251, and 252	350	0.7	Thioredoxin	Antisense	II
253	200	4.0	DAP-4	ND[a]	II
260	763	3.8	DAP-5	Sense	II

[a] ND, not determined.

is responsible for association with the cap binding protein eIF4E (31, 37). In this respect, DAP-5 can be regarded as a cellular gene whose product resembles the cleaved version of p220 which promotes cap-independent translation (45). In its N-terminal part (amino acids 110 to 361), DAP-5 protein has 63% similarity and 39% identity to the central region of mammalian p220. This region encompasses several highly conserved boxes of homology. The C-terminal part of DAP-5 is relatively less homologous to the mammalian p220 and therefore may possess some specific functions. Intriguingly, the rescued partial cDNA clone of DAP-5 conferred resistance to the IFN-γ-induced cell death, being expressed from the vector in the sense orientation. It was derived from the relatively less conserved C-terminal part of DAP-5 and directed the synthesis of a 28-kDa miniprotein. The relevance of DAP-5, the newly cloned p220 homolog, to possible changes in a cell's translational machinery during programmed cell death and growth arrest is discussed.

MATERIALS AND METHODS

Cell lines. HeLa human epithelial carcinoma cells were grown in Dulbecco modified Eagle medium (BioLab) supplemented with 10% fetal calf serum (Hyclone), 4 mM glutamine, 100 U of penicillin/ml, and 0.1 mg of streptomycin/ml. HeLa-tTA cells were grown in the presence of 200 μg of G-418/ml (22). Transfections of HeLa or HeLa-tTA cells were performed by the standard calcium phosphate technique. Recombinant human IFN-γ (3×10^7 U/ml) was purchased from PeproTech.

Isolation of DAP-5 cDNA and nucleotide sequence analysis. The radiolabeled cDNA insert from pTKO1-260 was used to screen an amplified λgt10 cDNA library prepared from poly(A)$^+$ RNA of K562 cells. Approximately 10^6 PFU was screened, and 40 positive clones were subjected to analysis of their insert sizes. Plaque hybridization was performed under stringent conditions. Two independent clones, one carrying the longest 3.8-kb cDNA insert and the other being 1.8 kb shorter, were chosen for further analysis. For 5′ walking, DAP-5's most 5′ 600 bp (*Eco*RI-*Sac*I fragment) was used to screen cDNA libraries from K562 and from human kidney cells. Approximately 10^6 PFU from each library was screened, and 12 and 5 positive clones from the K562 and the human kidney libraries, respectively, were further analyzed. The cDNA inserts were subcloned into the Bluescript vector (Stratagene). The sequencing of both strands was done by primer walking and was fully automated on an Applied Biosystems DNA 373A sequencer. Sequence uniqueness and relatedness were determined with FASTA (Genetics Computer Group [GCG] software package) at the nucleotide level and with the FASTA, PileUp (GCG), BLASTP (1), and PHD programs (47, 48) at the amino acid level.

Transfections and selection procedures. Two secondary polyclonal HeLa cell populations expressing the 763-bp DAP-5 cDNA fragment from the pTKO1 vector were generated. This was performed by the transfection of subconfluent monolayers of 1.5×10^6 HeLa cells with 40 μg of the corresponding plasmid (named pTKO1-260). In parallel, HeLa cells were transfected with a control vector, pTKO1-DHFR (13). Pools of 10^4 independent stable clones were generated from each transfection. The stable transfectants were maintained in the presence of 200 μg of hygromycin B (Calbiochem)/ml. Subconfluent monolayers of 1.5×10^6 HeLa-tTA cells were transfected with 15 μg of the pSBc-bl plasmid or the pSBc-bl plasmid carrying either fragment 260 (pSBc-bl-260) or its mutant derivatives (single- and triple-ATG mutants) and selected in the presence of either 10 or 50 μg of bleomycin/ml. Pools of 10^2 to 10^3 independent stable clones were generated from each transfection.

X-Gal staining. To detect LacZ activity, cells were fixed with 3% paraformaldehyde for 5 min, rinsed twice with phosphate-buffered saline, and stained for 3 h in X-Gal buffer, containing 77 mM Na_2HPO_4, 23 mM NaH_2PO_4, 1.3 mM $MgCl_2$, 1 mg of X-Gal (5-bromo-4-chloro-3-indolyl-β-D-galactopyranoside)/ml, 3 mM $K_3Fe(CN)_6$, and 3 mM $K_4Fe(CN)_6$. The reaction was stopped by addition of 70% ethanol. Photography was done under phase microscopy with Kodak Ektachrome 160T film.

In vitro translation of DAP-5 protein in reticulocyte lysate. The full-length cDNA insert or the fragment 260 variants cloned into the Bluescript vector (Stratagene) were used as templates for in vitro transcription from the T7 promoter. These RNAs were then translated in reticulocyte lysates (Promega) by conventional procedures, with [^{35}S]methionine (Amersham) as a labeled precursor. The reaction products were resolved by fractionation on a sodium dodecyl sulfate (SDS)–12.5% polyacrylamide gel, followed by salicylic acid amplification of the radioactive signal performed as described previously (30). ATG codons at positions 1785 to 1787, 2010 to 2012, or 2040 to 2042 were mutated by oligonucleotide-directed mutagenesis (ATG was converted into AAG, TTC, or ATC, respectively).

Preparation of antibodies and immunoblot analysis. The DAP-5 sequence corresponding to amino acids 522 to 776 of the coding region encompassed in fragment 260 was fused in frame to pGEX1 (GST260). Expression of the glutathione *S*-transferase (GST)-fused chimera was induced in *Escherichia coli* XL1-Blue with IPTG (isopropyl-β-D-thiogalactopyranoside). The GST-fused product purified on glutathione beads was used to immunize two rabbits. The antiserum was depleted of the anti-GST antibodies by passing it through CNBr-activated Sepharose beads (Pharmacia Biotech Inc.) coupled to GST. Affinity purification was then carried out on CNBr-activated Sepharose beads coupled to GST260. In several experiments the signal of the miniprotein in the HeLa cell transfectants was below detection limits.

HeLa-tTA cells that had been analyzed by Western blotting were harvested and lysed by boiling in sample buffer. The protein samples were fractionated by SDS–10% polyacrylamide gel electrophoresis and then transferred to a nitrocellulose filter (Schleicher & Schuell). The blots were reacted with the affinity-purified polyclonal antibodies (1:20 dilution), and immunodetection was done by the enhanced chemiluminescence detection system (Amersham Corp.).

Nucleotide sequence accession number. The DAP-5 accession number is X89713.

RESULTS

cDNA fragments rescued from cells surviving in the presence of IFN-γ can be classified into two functional groups. The response of HeLa cells to IFN-γ had two sequential phases. First, the cells stopped proliferating but still remained viable (the first 3 to 4 days). This was followed by a second phase of slow and asynchronous cell death that occurred over a period of several days. Cell death was characterized by a reduction in cell size, cytoskeletal disorganization, rounding up, and detachment from the plates; these events were followed by nuclear chromatin condensation with subsequent segmentation (5, 11). The original transfection-selection procedure for isolating functional cDNA fragments that convey resistance to IFN-γ was previously described in detail (11). Briefly, random cDNA fragments originating from HeLa cell mRNA were subcloned into the pTKO1 Epstein-Barr virus-based expression vector and were introduced into HeLa cells. The stable transfectants that survived after long-term double selection (28 days) with IFN-γ and hygromycin B were pooled, and the episomal DNAs were extracted. Each individual plasmid was then subjected to a second round of transfection. The plasmids that scored positively in the second round are listed in Table 1. They corre-

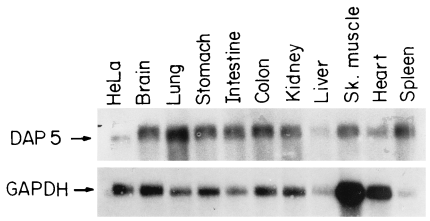

FIG. 1. Tissue distribution of DAP-5 mRNA. The tissue distribution of DAP-5 mRNA was determined by Northern blot analysis. Each lane contains 2 μg of poly(A)$^+$ RNA from different human tissues. This blot was probed with the 763-bp DAP-5 fragment (260). Glyceraldehyde-3-phosphate dehydrogenase (GAPDH) was used as a reference standard. Sk., skeletal.

spond to the thioredoxin and cathepsin D genes and to five novel genes named DAP genes.

Characterization of the IFN-γ resistance phenotypes which were generated by the rescued cDNAs indicated that they could be divided into two major subgroups. One type of resistance was conferred by transfections with the antisense cDNA fragments corresponding to DAP-1 (fragments 230, 254, 255, 258, and 264), DAP kinase (fragment 256), DAP-3 (fragment 259), and cathepsin D (fragment 229) (Table 1). Each of these eight cDNA fragments partially interfered with cytokine-induced cell death, whereas the cytostatic responses to IFN-γ appeared uninterrupted. As a consequence, a significant fraction of nondividing cells still remained viable during the first 2 weeks of IFN-γ treatment, as previously described in detail (11, 12, 30). The ability of these antisense cDNA fragments to protect cells exclusively from programmed cell death, without affecting growth arrest, provided the first indication that the corresponding cellular genes are positive mediators of cell death.

The second phenotype appeared to be more complex. It was generated by transfections of HeLa cells with the cDNA fragments corresponding to thioredoxin (fragments 241, 248, 251, and 252), DAP-4 (fragment 253), and DAP-5 (fragment 260) (Table 1). During the first 2 weeks of IFN-γ treatment, these polyclonal cell populations behaved similarly to the parental cells, both with respect to time kinetics and to the extents of growth arrest and programmed cell death. However, later on, at the time when a few resistant colonies appeared in the parental cells, there was around a 100-fold increase in the number of colonies that grew in the transfected cell populations. DAP-5, a subgroup II gene, was chosen for further analysis.

Cloning of DAP-5 cDNA and RNA expression studies. The nucleotide sequence of the 763-bp DAP-5 cDNA fragment, which conferred the aforementioned type of resistance to the IFN-γ treatment, did not reveal any significant homology to known genes when subjected to a homology search in the available databases. On Northern blots, a DAP-5 cDNA fragment hybridized in HeLa cells to a single mRNA transcript of 3.8 kb (Fig. 1; see also Fig. 5A, lane 1). The pattern of DAP-5 mRNA expression was examined in various human tissues. The DAP-5 mRNA was found to be widely expressed, with high abundance in all tissues tested (Fig. 1). This 3.8-kb DAP-5 mRNA appeared as a single transcript also when the full-length cDNA was used as a probe, and its levels were not modulated by IFN-γ (not shown).

In order to isolate the full-length cDNA clone, the 763-bp cDNA fragment was used as a probe to screen a K562 λgt10 cDNA library. Two independent phage clones carrying cDNA inserts of 3,785 and 2,032 bp were analyzed. The shorter clone overlapped the 3′ part of the longer clone, and both extended to their poly(A) tails. Two cDNA libraries derived from K562 and human kidney cells were further screened with a cDNA fragment encompassing the most 5′ region of the 3,785-bp clone. All the positive clones (12 clones from the K562 library and 5 clones originating from the human kidney library) had identical 5′ ends that coincided with the starting point of the original 3,785-bp cDNA.

A single, long open reading frame (ORF) with the potential to code for a protein with a maximal length of 940 amino acids (from positions 201 to 3020) was identified within this 3,785-bp-long cDNA (Fig. 2). Although an initiator AUG codon was not found at the beginning of this ORF, in vitro translation assays in reticulocyte lysates confirmed that the RNA transcribed from this cDNA directed the synthesis of a protein approximately 97 kDa in size (see Fig. 7A, lane 2). In rare cases, codons other than AUG can function as initiators (3). This probably also occurs with DAP-5, as demonstrated by Imataka et al., who have cloned this gene independently and proved that the GUG codon at position 299 serves as the initiator codon (26). The 5′ untranslated region (UTR) preceding the aforementioned initiator GUG codon encompasses two polypyrimidine tracts (Fig. 2).

The deduced amino acid sequence predicts that the DAP-5 protein is a novel homolog of eIF4G. A homology search of the available databases revealed that the predicted 940-amino-acid protein was homologous to eIF4G (p220) of various species, including human, rabbit, *Caenorhabditis elegans*, *Saccharomyces cerevisiae*, and wheat (Fig. 3A) (overall, DAP-5 has 26.8% identity and 48.2% similarity to human p220). Thus, we had identified a new member of the eIF4G gene family.

Initiation factor 4G, also known as p220, is part of the cap binding complex (for a review, see reference 39). The N-terminal part of eIF4G binds eIF4E, the cap binding protein, whereas the regions that bind eIF3 and eIF4A lie further downstream (31, 37). Upon viral infection, p220 is cleaved by specific viral proteinases (29, 32). This cleavage separates the N-terminal eIF4E binding domain from the rest of the molecule. Due to this cleavage, cap-dependent translation is inhibited while cap-independent translation of viral RNAs, which are naturally uncapped, proceeds via their internal ribosome entry sites (IRES).

A few interesting features emerged from the alignment of DAP-5 with human and rabbit p220 variants (which are each approximately 1,300 amino acids in size) as well as with the yeast and the wheat eIF4G homologs. The first striking notion was the lack of an eIF4E binding motif in DAP-5 protein. The site on p220 that specifically associates with eIF4E was previously mapped to amino acids 414 to 426 and 413 to 425 in the human and rabbit p220 proteins, respectively (37). Within this region, a conserved motif of three hydrophobic amino acids at five distinct positions (YXXXFLLXF) was defined. Some of these amino acids, including a tyrosine residue (Y416), were proven to be essential for eIF4E binding. The motif seems to be truncated in the deduced ORF shown in Fig. 2 (amino acids 8 to 12) and actually is not included in the protein which starts from GUG at position 299 (26). Thus, it is most likely that DAP-5 does not bind eIF4E.

The N-terminal part of DAP-5 starting from amino acid 110 was found to be highly homologous to the central regions of eIF4G proteins from various species and contained several boxes of homology that are conserved among all eIF4G family members (Fig. 3A). When a stretch of 240 amino acids from this region (positions 111 to 351) was subjected to a homology search with the BLASTP 1.4.8MP program (1) (matrix BLOSOM62), the eIF4G proteins from the various species scored high, with sum probabilities ranging from $2.3e^{-48}$ to $3.6e^{-21}$. In contrast to the N-terminal part of DAP-5, its C-terminal part

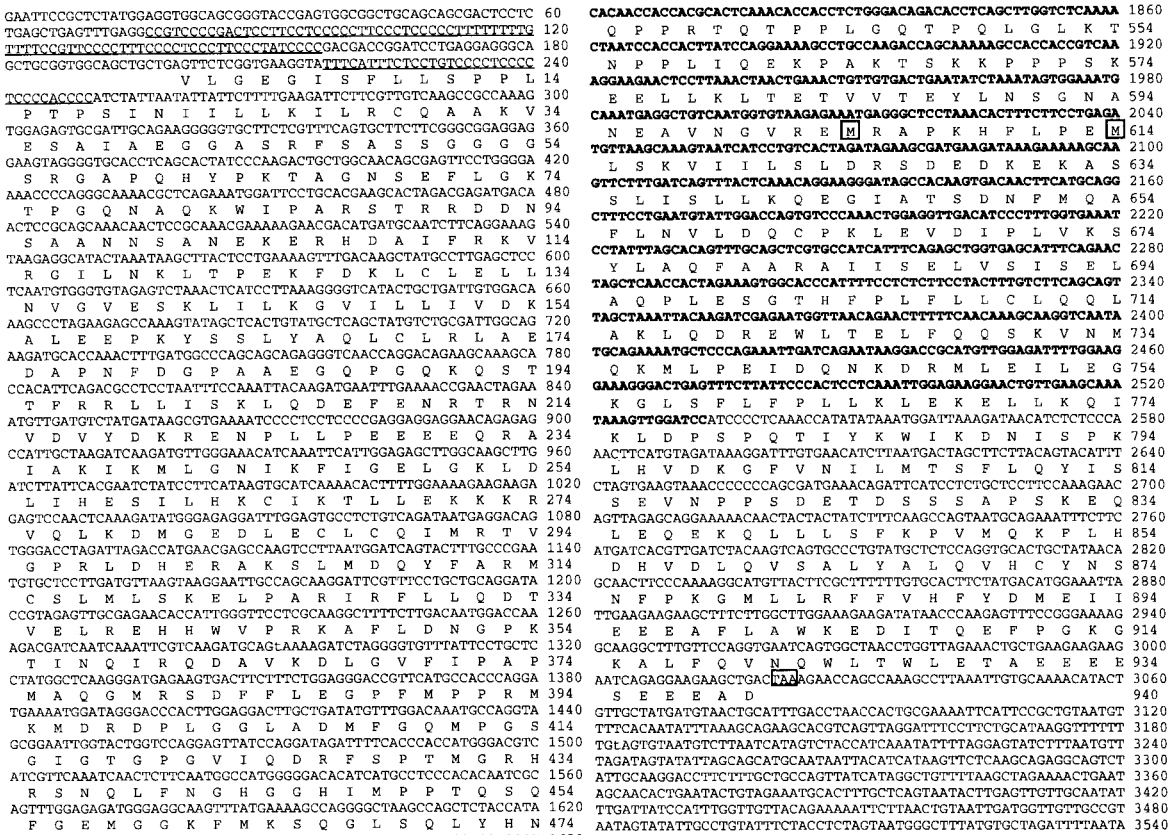

FIG. 2. Nucleotide and deduced amino acid sequences of the DAP-5 cDNA. The sequence of the 3.8-kb full-length DAP-5 clone is shown. Polypyrimidine tracts are underlined. The predicted amino acids included in the miniprotein are marked in boldface letters. The TAA stop codon and the polyadenylation signal, as well as the potential initiator codons of the miniprotein, are boxed.

showed relatively less homology to the corresponding regions in human, rabbit, nematode, and wheat eIF4G proteins (Fig. 3B and 4 and as will be further discussed). Interestingly, the two yeast homologs, p150 and p130, completely lacked this less-conserved C-terminal region (Fig. 3B). The N-terminal and C-terminal parts of DAP-5 are separated by a hinge-like region (between amino acids 360 and 395). When aligned separately, human and rabbit p220 variants are almost identical except for the small stretch of poorly conserved amino acids mapped to positions 809 to 854 in the human protein (corresponding to positions 360 to 395 in DAP-5) (Fig. 4). The high degree of conservation in the C-terminal portion between human and rabbit p220 raises the possibility that it represents a functional domain within p220 that is separated from the N-terminal conserved regions by a hinge-like stretch of nonconserved amino acids. This C-terminal domain is completely absent in the yeast p220 homologs and thus may possess a function that was acquired later on in evolution.

From the sequence analysis it was found that the 763-bp DAP-5 cDNA fragment that was rescued as an element which conferred the type II growth resistance to IFN-γ was inserted into the episome in the sense orientation. All the other studied DAP genes isolated so far in our laboratory were selected as antisense cDNA fragments 200 to 370 bp in size (Table 1). The DAP-5 cDNA fragment was the longest and the first functional cDNA clone selected that was expressed in the sense direction. The RNA transcribed from the expression vector comprised part of the coding region of DAP-5, extending between amino acids 522 and 776 (Fig. 2). It carried a single potential ORF, which was identical to that of the full-length DAP-5, suggesting that it may code for a miniprotein corresponding to the less-conserved C-terminal portion of DAP-5.

When the deduced amino acid sequence of the miniprotein (amino acids 522 to 776) was subjected to a homology search with the above-mentioned BLASTP 1.4.8MP program (1) (matrix BLOSOM62), various eIF4G proteins scored with sum probabilities of 1.3 to $3.3e^{-6}$, which differ by several orders of magnitude from the scores obtained when the conserved N-terminal region was subjected to such analysis ($2.3e^{-48}$ to $3.6e^{-21}$). Moreover, when the putative miniprotein and the corresponding region from the human p220 were subjected to the PHD search (47, 48), which predicts protein secondary structures, a marked difference was revealed. The N-terminal part (the first 100 amino acids) of this putative miniprotein was composed mostly of loops, while the corresponding region in p220 was mostly helical in structure (Fig. 4). Thus, the C-terminal region of DAP-5, which corresponds to the miniprotein, differs to a substantial extent from the C-terminal regions of the eIF4G family members, as can be seen from its deduced amino acid sequence and predicted secondary struc-

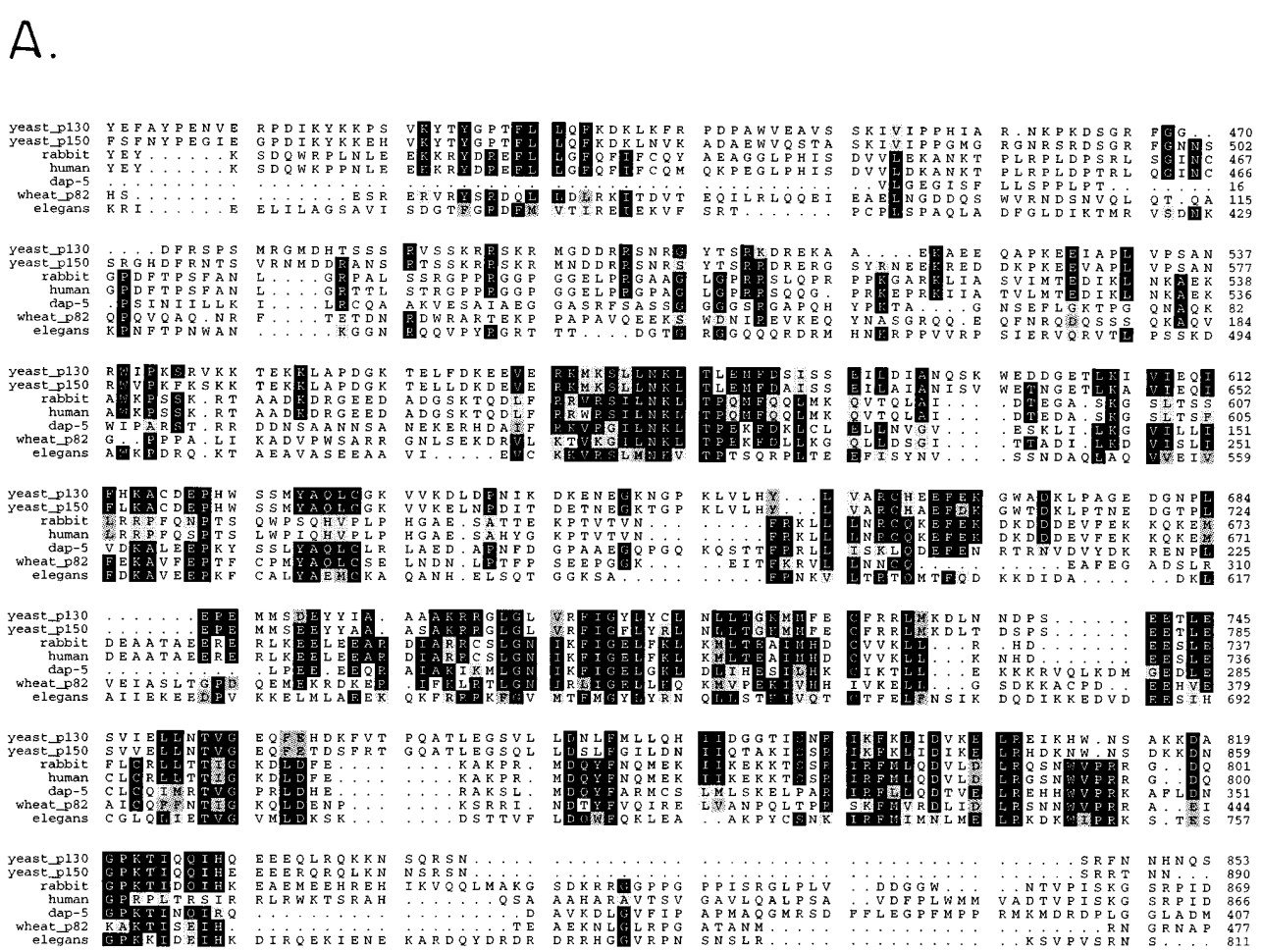

FIG. 3. Alignment of DAP-5 deduced amino acid sequence with those of the eIF4G proteins from various species. The accession numbers of the aligned sequences are as follows: yeast p130, P39936; yeast p150, P39935; rabbit p220 homolog, P41110; human p220, Q04634; wheat p82, Q03387; and nematode p220 homolog, Z49968. The sequences were aligned with the PileUp program of the GCG sequence analysis software package, version 8.1 (gap creation penalty, 3.00; extension penalty, 0.1). Identical and conserved amino acids are in filled and shaded boxes, respectively. (A) Regions of high homology containing several highly conserved boxes. (B) The C-terminal part of DAP-5, encompassing the miniprotein region, aligned with the corresponding regions of the various eIF4G homologs.

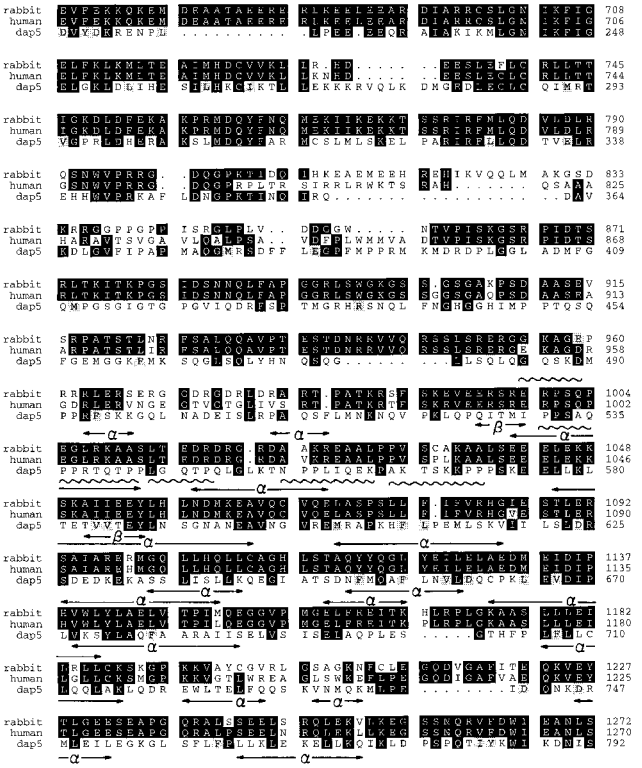

FIG. 4. Comparison of the primary and secondary structures of DAP-5 with those of the human and rabbit homologs of p220. The sequences were aligned with the PileUp program of the GCG sequence analysis software package, version 8.1 (gap creation penalty, 3.00; extension penalty, 0.1). Identical and conserved amino acids are in filled and shaded boxes, respectively. The secondary structure of the miniprotein and the corresponding region of human p220 were predicted with the PHD program (48). Only stretches of a minimum of 5 amino acids with a reliability index of prediction of 8 or 9 are marked. Loops are marked by wavy lines, and α helices (α) and β sheets (β) are marked by arrows. The symbols corresponding to human p220 and to the miniprotein appear above and below the aligned sequences, respectively.

ture, suggesting that it might possess unique functional properties.

Expression of the DAP-5 cDNA fragment (260) exerts a dual effect on HeLa cells. The pTKO1 construct containing DAP-5 cDNA fragment 260 was transfected (in duplicate) into HeLa cells to generate two stable polyclonal cell populations (named 260-t1 and 260-t2). A control polyclonal HeLa cell population (designated DHFR-t1) was obtained by transfection of the pTKO1 vector carrying the dihydrofolate reductase gene. These three transfected cell cultures were subjected to long-term treatment with IFN-γ. As shown in Fig. 5B, there was a 100- to 200-fold increase in the number of growing colonies in the 260-t1 and 260-t2 cell cultures compared to that of the DHFR-t1 cell population. This means that the total number of colonies which were rescued from the inhibitory effects of IFN-γ by this cDNA fragment corresponded to only 0.1 to 1% of the initial cell population. This pattern, in which only a small fraction of cells were protected from programmed cell death, was very similar to the effect that was conferred by the anti-thioredoxin RNA (Fig. 4 in reference 13) and by fragment 253 (unpublished results), all classified in subgroup II.

The size of exogenous DAP-5 RNAs in the 260-t1 and 260-t2 transfectants was 1.7 kb [consisting of 763 bases of the cDNA insert and 800 bases of sequences derived from the expression cassette (13) and the poly(A) tail]. The expression levels of the exogenous RNA were much lower than those of the endogenous 3.8-kb transcript (Fig. 5A). These low levels stand in sharp contrast to those of the eight plasmids of subgroup I, whose RNA products accumulated in HeLa cells in great excess of the endogenous mRNA transcripts (11, 12, 30). A more detailed comparison between the two subgroups was performed by hybridization of Northern blots, containing RNA from the different HeLa transfectants, with a common DNA probe derived from the pTKO1 vector. As shown in Fig. 5C, under conditions where the RNA expressed from the pTKO1-230 vector (containing the antisense fragment of DAP-1) (11) gave a strong signal, the RNA transcribed from fragment 260 was still below detection limits. Similar low levels of RNA were expressed from two other subgroup II cDNA fragments carried

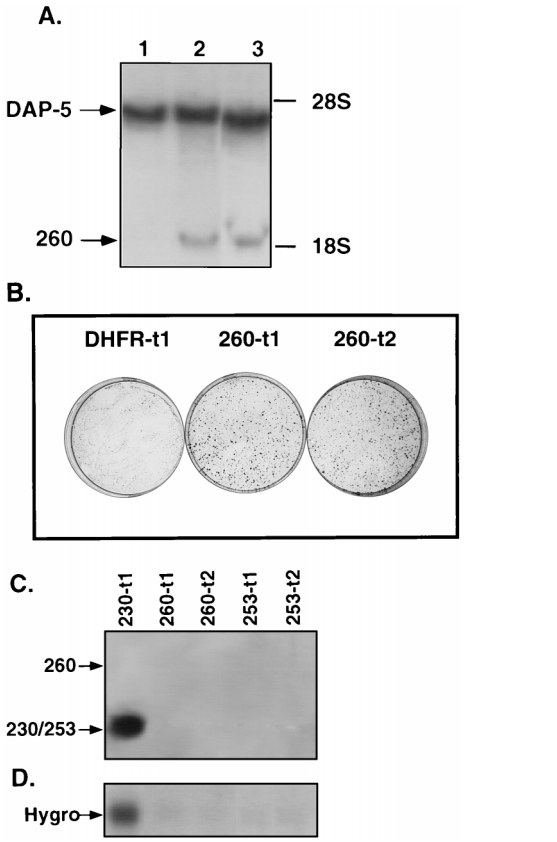

FIG. 5. The 763-bp DAP-5 fragment is expressed in HeLa cells at very low levels compared to those of the subgroup I cDNA fragment. (A) Northern blot analysis of RNA from pTKO1-260- or pTKO1-DHFR-transfected cells. RNAs were extracted from the indicated HeLa cells. The Northern blot containing 20-μg samples of total RNA was hybridized with the 763-bp DAP-5 fragment (260). Lanes: 1, DHFR-t1; 2, 260-t1; 3, 260-t2. (B) IFN-γ-resistant phenotype of HeLa cells transfected with pTKO1-260. HeLa cells were transfected with either the control vector pTKO1-DHFR or the isolated plasmid pTKO1-260. Pools of more than 10^4 independent clones were first selected with hygromycin B to generate polyclonal populations of stably transfected cells. These pools were plated in 9-cm-diameter plates (100,000 cells per plate) and double selected with IFN-γ (1,000 U/ml) and hygromycin B (200 μg/ml). After 4 weeks of selection, the cells were stained with crystal violet. In the absence of IFN-γ, these plates reached confluency after 4 days. (C) Comparison of the expression levels of RNAs from subgroups I and II. 260-t1 and 260-t2 represent the same extracts used in panel A. The Northern blot containing 20-μg samples of RNA was hybridized with the *Bgl*II-*Bam*HI fragment containing the simian virus 40 splice and polyadenylation signal (13) which is part of the simian virus 40 promoter-driven, fragment 260-containing mRNA expressed from the episome. (D) The contents of the lanes are the same as in panel C, but they were hybridized with a probe recognizing the hygromycin B (Hygro) resistance gene driven by the TK promoter (13).

by the same vector, thioredoxin (13) and DAP-4 (fragment 253 [Fig. 5C]). Thus, the low levels of the ectopically expressed RNA in the established polyclonal populations provided a second characteristic feature of subgroup II cDNA fragments. This result could reflect either RNA instability or, alternatively, the selection of transfectants with low copy numbers of episomes. The latter seemed to be true, since a transcript common to all the transfectants—the mRNA expressed from the hygromycin B resistance gene placed within pTKO1 under the control of the thymidine kinase promoter—paralleled the expression levels of the inserted cDNA fragments (Fig. 5D). Thus, we postulated that during the establishment of the polyclonal cell populations in the presence of hygromycin B only, cells containing low copy numbers of the pTKO1-260 episomes gained a significant growth advantage.

To further pursue this possibility, we tested whether indeed high levels of expression of the DAP-5 partial cDNA were incompatible with continuous cell growth. For this purpose, we constructed a polycistronic vector (pSBc-bl-260) which directed the expression of a bicistronic message containing both cDNA fragment 260 and the SH-LacZ protein which directs the synthesis of a fused protein conferring resistance to bleomycin and producing β-galactosidase (Cayla). LacZ was used as a marker to evaluate the bicistronic mRNA levels in individual cells. cDNA fragment 260 was translated in a cap-dependent manner, whereas the SH-LacZ fused gene was placed downstream of the poliovirus IRES. Since IRES-directed translation is less efficient than the cap-dependent one, high levels of bicistronic message had to be expressed in order to allow the survival of cells under bleomycin selection. This imposed high levels of expression from fragment 260 in these cells. We found that transfections of HeLa-tTA cells with the pSBc-bl-260 vector did not yield stable clones in the presence of 50 μg of bleomycin/ml, while transfection with the control vector lacking the insert (pSBc-bl) generated clones readily. At lower concentrations of the drug (10 μg of bleomycin/ml), small clones did arise after transfections with the pSBc-bl-260 vector; yet, they slowly died thereafter. This indicated that high levels of expression from cDNA fragment 260 were lethal to cells and that fragment 260-dependent cell death displayed a pattern of slow killing. The expression levels of the bicistronic mRNA and hence of fragment 260 that were permissive for cell growth were not sufficient for conferring bleomycin resistance, and therefore the drug had to be removed in order to enable further analysis of these transfectants. The β-galactosidase activity served to quantify expression on a single-cell basis in surviving cells. In the pSBc-bl-260-transfected cultures, the extent of blue staining was very weak in all the cells on the plate. In contrast, the polyclonal cell populations obtained from transfection with the control vector and selected under identical conditions showed a strong pattern of β-galactosidase staining, exceeding by many fold the pattern in pSBc-bl-260 transfectants (Fig. 6A). Together, the reduced cloning efficiency and the weak β-galactosidase activity in the surviving cells proved that there was selection against high-level expression of cDNA fragment 260. We concluded that expression from the rescued DAP-5 cDNA fragment had a dual effect: at low levels it conferred IFN-γ resistance (a property that led to its functional cloning), and at higher levels it was toxic and not permissive to continuous cell growth.

Fragment 260 directs the expression of a functional miniprotein. Three AUG codons that could serve as potential initiators of translation were found in the ORF of fragment 260. One was located at the beginning of the fragment and may be able to initiate the synthesis of a 28-kDa protein; the two others were located 85 and 75 amino acids downstream and

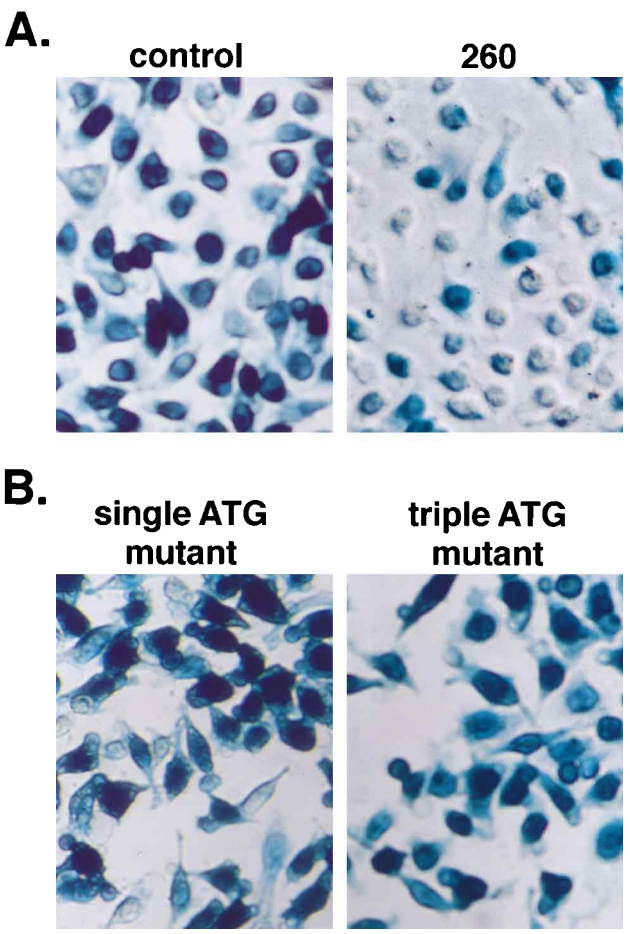

FIG. 6. β-Galactosidase activity assays of HeLa-tTA cells transfected with the 763-bp DAP-5 fragment or its mutated versions. Stable polyclonal populations transfected with the pSBc-bl vector (control), with pSBc-bl-260 (260), or with the pSBc-bl vector harboring either the single or the triple ATG fragment 260 mutant were established by selection with 10 μg of bleomycin/ml. After 2 weeks the drug was removed and cultures were further expanded. Growing cells were fixed with 3% paraformaldehyde for 5 min, rinsed twice with phosphate-buffered saline, and checked for β-galactosidase activity with X-Gal as a substrate. Photography was done under phase microscopy with Kodak Ektachrome 160T film.

may give rise to 20- and 18.8-kDa proteins, respectively (Fig. 2). In vitro translation of the RNA transcribed from the 763-bp DAP-5 cDNA fragment generated a doublet of proteins that had an approximate size of 28 kDa (Fig. 7A, lane 3). A missense mutation in the first ATG codon, which did not affect the two downstream ATG codons, completely eliminated the synthesis of these two closely migrating proteins. A missense mutation in the next two ATG codons did not interfere with the translation of the doublet; a triple mutation in all potential initiation codons completely prevented protein translation, as did the single mutation in the first ATG codon (Fig. 7A, lanes 4 to 6, respectively). Thus, we concluded that the rescued cDNA fragment could drive the expression of a miniprotein starting at Met 529. This miniprotein was also detected in the aforementioned population of HeLa cells that had been transfected with the pSBc-bl vector harboring fragment 260. As shown in Fig. 7B, affinity-purified polyclonal antibodies raised against the recombinant miniprotein identified two closely migrating proteins with an approximate size of 28 kDa exclusively

in the cells transfected with pSBc-bl-260, not in cells transfected with the empty vector.

We then asked whether the biological effects conferred on the transfected cells by fragment 260 resulted from expression of the miniprotein. For that purpose, we subcloned each of the two mutant cDNA fragments which failed to be translated in vitro into the pSBc-bl vector. In contrast to the transfections with the protein expressing the DAP-5 fragment, polyclonal cell populations obtained with the mutant fragments were established in the presence of bleomycin, with an efficiency similar to that of the control vector. In addition, the β-galactosidase activity in these transfectants was as high as in the cells transfected with the control vector (Fig. 6B). Thus, high levels of expression of the mutant DAP-5 cDNA fragment proved to be compatible with continuous cell growth. The translated miniprotein is therefore responsible for the cellular effects that the rescued DAP-5 fragment exerts on cells.

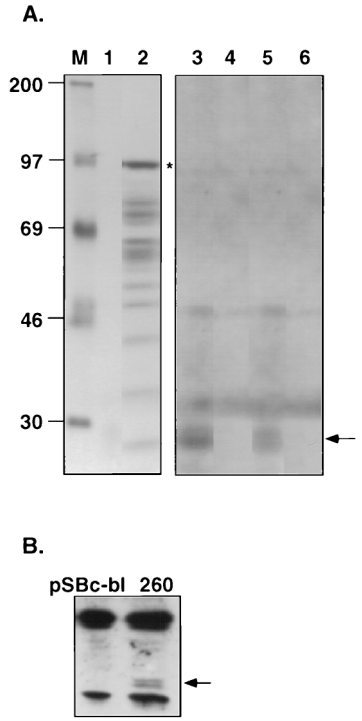

FIG. 7. In vitro translation of the 763-bp DAP-5 fragment and immunoblot analysis of the miniprotein in cells expressing fragment 260. (A) In vitro translation of RNA transcribed from the Bluescript vector harboring various DAP-5 versions was done in rabbit reticulocyte lysates. The resulting ^{35}S-labeled proteins were fractionated on SDS–12.5% polyacrylamide gels. The positions of radioactive molecular mass markers (in kilodaltons) (Amersham) are marked to the left of lane M. Lanes: 1, nonprogrammed rabbit reticulocyte lysates; 2, full-length 3.8-kb DAP-5 clone (the position of the full-length DAP-5 protein is indicated by the asterisk); 3, 763-bp DAP-5 fragment (260); 4, mutated fragment 260 (ATG at position 1785 was converted to AAG [single ATG mutant]); 5, mutated fragment 260 (ATG at position 2010 was converted to TTC, and ATG at position 2040 was converted to ATC); 6, triple ATG mutant harboring all the above-mentioned mutations. The position of the translated miniprotein is marked by an arrow; the additional higher bands are nonspecific background that often appears also in nonprogrammed reticulocyte lysates. (B) HeLa-tTA cells transfected with either the pSBc-bl vector or the pSBc-bl vector harboring fragment 260 (260) were lysed and fractionated on an SDS–10% polyacrylamide gel, blotted onto nitrocellulose, and reacted with affinity-purified polyclonal antibodies (1:20 dilution) raised against a GST-fused recombinant product. The arrow points to the position of the DAP-5 miniprotein-specific doublet that had an approximate size of 28 kDa.

DISCUSSION

The role of cap-dependent translational control in the regulation of cellular proliferation was demonstrated by several systems (51). The cap associates with eukaryotic initiation factor 4F (16, 24, 54, 58), a protein complex which consists of three polypeptides: eIF4E (a 25-kDa cap binding protein) (52, 53), eIF4G (p220), and eIF4A (a 46-kDa RNA helicase). eIF4E, the least abundant of all translation initiation factors (14, 25), is regarded as the rate-limiting factor in the cap binding complex and the main target for regulation (51). It has been reported, in this respect, that overexpression of eIF4E led to deregulation of cell growth in HeLa cells (9) and to the transformation of rodent cells (8, 33, 34). Moreover, growth factors and mitogens were shown to increase the activity of eIF4E, either by its phosphorylation (19, 42, 43) or by dissociating the 4E binding protein 1 inhibitor from eIF4E via phosphorylation of the inhibitor (35, 46). The latter increased the cap-dependent translation of RNAs transcribed from growth-promoting genes that possess an unusually long and highly structured 5′ UTR (7, 8, 38, 50). Conversely, the rapamycin-induced reduction of 4E binding protein 1 phosphorylation, which inhibited eIF4E activity and cap-dependent translation, was correlated with a G_1 type of cell cycle arrest (2).

In contrast to the aforementioned studies which dealt with the role of protein translation in cell growth control, very little is known about the regulation of the translation machinery during programmed cell death and its possible role in controlling apoptotic processes. While several rapid apoptotic processes can be executed in the continuous presence of cycloheximide (41), in other systems the process develops much more slowly (e.g., in the IFN-γ–HeLa cell system which was used in this work) or is even inhibited by cycloheximide (10, 59). This may imply the involvement of critical changes in translation. One of the studied examples is the metamorphic death of the tobacco hornworm labial glands. In this system, a sharp drop in protein synthesis, coupled to selective up regulation of a few other specific proteins, was among the earliest of the changes occurring in the cells that were prone to die (59). A similar change in the pattern of translation was found in nerve growth factor-deprived sympathetic neurons (10). There are two examples of translational selectivity that were addressed mechanistically; one example was observed after heat shock, and the other was observed upon viral infection. In the heat shock system, translation of the majority of cellular proteins is suppressed by the elevated temperature, due to a reduction of eIF4E function, while the synthesis of heat shock proteins remains refractory to this change (15). Upon viral infection, there is a shutoff of the majority of the cellular genes whose translation is cap dependent, while viral RNAs are translated via ribosome entry sites in a cap-independent manner. The viral protease cleavage sites in p220 are located downstream from the eIF4E binding motif, thus generating a polypeptide which binds only to eIF4A and eIF3 and therefore fails to direct cap-dependent translation. Although the notion has circulated for a long time, in a recent paper (45) it was clearly demonstrated that the C-terminal part of eIF4G, which binds eIF3 and eIF4A, is necessary to support cap-independent translation.

In light of the different patterns of translational regulation in cell growth and viral infection, the identification of DAP-5 as a novel, shorter homolog of p220 was intriguing. Moreover, the notion that this gene was rescued by a functional assay that was aimed at isolating cell death genes introduced an important dimension to the function of this protein. The sequence analysis indicated that this novel homolog, while retaining the central conserved region of eIF4G proteins, lacked the N-

terminal part that is present in mammalian, wheat, and yeast eIF4G proteins and that contains the eIF4E binding motif. By that means, the full-length DAP-5 protein structurally resembled the cleaved product of p220. Moreover, the most C-terminal region of DAP-5 displayed a reduced degree of homology to p220, as reflected by its amino acid sequence and deduced secondary structure, suggesting that it may possess unique biochemical and functional properties.

Three main findings described in this paper should be considered together in order to understand the possible cellular role of DAP-5. The first is the intriguing finding that the rescued cDNA fragment was oriented within the original expression vector in the sense direction, and in this orientation it directed the synthesis of a miniprotein. This 28-kDa miniprotein represents part of the DAP-5 protein and thus may either function as a dominant-negative mutant, opposing the effect of the full-length protein, or, alternatively, mimic the effect of the full-length protein. In light of the fact that the other eIF4G homologs serve as the scaffold for assembling several initiation factors that direct ribosomes to RNA, it is likely that the miniprotein functions in a dominant-negative manner. Thus, it may counteract the function of endogenous DAP-5 by titrating out a putative protein which binds the C-terminal region of DAP-5.

The second finding is that overexpression of the DAP-5 miniprotein was lethal to HeLa cells. As a consequence, only low-level expressors of the DAP-5 cDNA fragment were selected by the transfections with the original episomal-based vector or with the bicistronic vector. If indeed this fragment functions exclusively as a dominant-negative inhibitor of DAP-5, this means that a complete functional shutoff of endogenous DAP-5 was not compatible with continuous HeLa cell growth and, hence, that DAP-5 has a vital role in growing HeLa cells.

The third point relates to the protective effect against death conveyed by the DAP-5 partial cDNA fragment, the feature which served as the basis for the fragment's functional cloning. The typical pattern, in which only a very small fraction of cells (between 0.1 and 1%) was protected from cell death, was also characteristic of the antithioredoxin transfectants (13), classified in the same functional subgroup. High levels of antisense thioredoxin which resulted in a complete shutoff of thioredoxin expression were also lethal, leading to a situation similar to that obtained with overexpression of DAP-5 miniprotein, i.e., selection of low-level expressors. Thus, among the stable transfectants, which express on average low levels of the cDNA, only a minor fraction of cells had amounts of either antithioredoxin or the DAP-5 miniprotein sufficient for interfering with IFN-γ-induced cell death. The rest of the hygromycin B-resistant cell population expressed lower levels, much below the minimal threshold that might have functional significance.

An attractive interpretation which considers all the three findings together is that the endogenous full-length DAP-5 protein may have a dual function in cells. On the one hand, its function may be essential for continuous cell viability under steady-state growth conditions, and therefore a complete functional block was lethal to cells. On the other hand, it may have a specific role during programmed cell death, since partial reduction in DAP-5 function, which was still growth permissive, appeared to be beneficial for cells exposed to an apoptotic stress. A similar situation involving a concentration-dependent dual effect was already established with respect to the intracellular levels of superoxides. While high levels were lethal to cells (a scenario that may develop in the complete absence of thioredoxin), intermediate levels of superoxides protected cells from various apoptotic stimuli (4).

The most important challenge in the near future is to study the biochemical features of DAP-5, putting a particular emphasis on its C-terminal part, and to correlate them with the aforementioned cellular functions. In addition, the role of the full-length protein should be elucidated by approaches such as knockout of the gene as well as studies of the regulation of its expression and function after different apoptotic insults. While no stimulatory effects by IFN-γ were detected on the level of mRNA expression, other levels of regulation should be considered. For instance, a long polypyrimidine stretch was found in the 5′ UTR of DAP-5. Polypyrimidine tracts are usually found in IRES (27) and in the 5′ UTRs of genes that are translationally regulated, such as those encoding the ribosomal proteins (see reference 40). The ORFs of human p220 (58) and of the yeast eIF4G homolog p150 (23) are also preceded by polypyrimidine stretches, and in the case of p220 it was recently shown that its 5′ UTR can direct internal initiation (21). This might imply that DAP-5 can be translationally regulated under certain conditions.

It has been shown by Imataka et al. (26) that this novel p220 homolog binds eIF3 and eIF4A and fails to bind eIF4E, as predicted by its primary structure (Fig. 3). Hence, the structural and biochemical resemblance of DAP-5 to the virally induced cleaved product of p220 raises two possible working models concerning the DAP-5 mode of action that should be addressed experimentally. According to one working model, DAP-5 may titrate out eIF3 and eIF4A and thus may reduce both cap-dependent and cap-independent translation. This model is consistent with the finding that overexpression of the full-length DAP-5 gene results in the inhibition of cap-dependent and cap-independent translation (26, 34a). In this scenario, DAP-5 protein expression or function should be tightly regulated since, as we had shown, the mRNA is abundantly expressed in growing cells. According to this first scenario, the rescued partial DAP-5 cDNA clone that is situated downstream from the highly conserved region of the DAP-5 protein could exert its protective effects by preventing DAP-5 activation.

The second working model implies that rather than acting as a passive titrator, the novel p220 homolog may have an active, positive role during programmed cell death. For instance, it may promote the translation of a still unidentified subset of mRNAs whose products are elevated during programmed cell death (59). In this scenario, cap-dependent translation could decline during IFN-γ-induced cell cycle arrest (which precedes the phase of cell death) by the previously discussed modulations of eIF4E that occur in growth arrest or following heat shock. Under these conditions, preexisting DAP-5 (or death-activated DAP-5) may stimulate the translation of a specific subset of RNAs in a cap-independent manner and thus may contribute to the apoptotic process, which can be regarded as part of the IFN-γ-induced cellular defense mechanisms against viral spread. According to each model, an important functional region should reside in the most C-terminal part of the DAP-5 protein, encompassing the miniprotein. To date, several cap-independent cellular genes have been identified (36, 44, 49, 56). From the data demonstrated by Imataka et al. (26) and results of experiments conducted in our laboratory (34a), it is concluded that DAP-5 cannot serve as a functional initiation factor of the encephalomyocarditis virus and poliovirus IRES. It is possible though that these IRES sequences are not natural targets of DAP-5, which possesses additional features that restrict its activity to a certain subset of mRNAs. This model therefore implies that DAP-5 may be responsible for a selective cap-independent translation of putative cell viability and

cell death genes and that the selectivity is mediated by its C-terminal portion.

ACKNOWLEDGMENTS

We thank Elena Feinstein for helpful discussions and for reading the manuscript. We also thank Orna Stein for helpful discussions, Nahum Sonenberg for sharing unpublished results, and Eli Cnaani for providing the K562 cDNA library.

This work was supported by the Israel Science Foundation, which is administered by the Israel Academy of Sciences and Humanities. A.K. is the incumbent of the Helena Rubinstein Chair of Cancer Research.

REFERENCES

1. **Altschul, S. F., W. Gish, W. Miller, E. W. Myers, and D. J. Lipman.** 1990. Basic local alignment search tool. J. Mol. Biol. **215:**403–410.
2. **Beretta, L., A. C. Gingras, Y. V. Svitkin, M. N. Hall, and N. Sonenberg.** 1996. Rapamycin blocks the phosphorylation of 4E-BP1 and inhibits cap-dependent initiation of translation. EMBO J. **15:**658–664.
3. **Boeck, R., and D. Kolakofsky.** 1994. Positions +5 and +6 can be major determinants of the efficiency of non-AUG initiation codons for protein synthesis. EMBO J. **13:**3608–3617.
4. **Clement, M. V., and I. Stamenkovic.** 1996. Superoxide anion is a natural inhibitor of FAS-mediated cell death. EMBO J. **15:**216–225.
5. **Cohen, O., E. Feinstein, and A. Kimchi.** DAP-kinase is a Ca^{2+}/calmodulin-dependent, cytoskeletal associated protein kinase, with cell death-inducing functions that depend on its catalytic activity. EMBO J., in press.
6. **Darnell, J. E., Jr., I. M. Kerr, and G. R. Stark.** 1994. Jak-STAT pathways and transcriptional activation in response to IFNs and other extracellular signaling proteins. Science **264:**1415–1421.
7. **Darveau, A., J. Pelletier, and N. Sonenberg.** 1985. Differential efficiencies of in vitro translation of mouse c-myc transcripts differing in the 5′ untranslated region. Proc. Natl. Acad. Sci. USA **82:**2315–2319.
8. **De Benedetti, A., B. Joshi, J. R. Graff, and S. G. Zimmer.** 1994. CHO cells transformed by the initiation factor eIF-4E display increased c-myc expression but require overexpression of Max for tumorigenicity. Mol. Cell. Differ. **2:**347–371.
9. **De Benedetti, A., and R. E. Rhoads.** 1990. Overexpression of eukaryotic protein synthesis initiation factor 4E in HeLa cells results in aberrant growth and morphology. Proc. Natl. Acad. Sci. USA **87:**8212–8216.
10. **Deckwerth, T. L., and E. M. Johnson, Jr.** 1993. Temporal analysis of events associated with programmed cell death (apoptosis) of sympathetic neurons deprived of nerve growth factor. J. Cell Biol. **123:**1207–1222.
11. **Deiss, L. P., E. Feinstein, H. Berissi, O. Cohen, and A. Kimchi.** 1995. Identification of a novel serine/threonine kinase and a novel 15-kD protein as potential mediators of the gamma interferon-induced cell death. Genes Dev. **9:**15–30.
12. **Deiss, L. P., H. Galinka, H. Berissi, O. Cohen, and A. Kimchi.** 1996. Cathepsin D protease mediates programmed cell death induced by interferon-γ, FAS/APO-1 and TNF-α. EMBO J. **15:**3861–3870.
13. **Deiss, L. P., and A. Kimchi.** 1991. A genetic tool used to identify thioredoxin as a mediator of a growth inhibitory signal. Science **252:**117–120.
14. **Duncan, R., S. C. Milburn, and J. W. B. Hershey.** 1987. Regulated phosphorylation and low abundance of HeLa cell initiation factor eIF-4F suggest a role in translational control. Heat shock effects on eIF-4F. J. Biol. Chem. **262:**380–388.
15. **Duncan, R. F.** 1996. Translational control during heat shock, p. 271–294. *In* J. W. B. Hershey, M. Mathews, and N. Sonenberg (ed.), Translational control. Cold Spring Harbor Laboratory Press, Cold Spring Harbor, N.Y.
16. **Edery, I., M. Humbelin, A. Darveau, K. A. Lee, S. Milburn, J. W. B. Hershey, H. Trachsel, and N. Sonenberg.** 1983. Involvement of eukaryotic initiation factor 4A in the cap recognition process. J. Biol. Chem. **258:**11398–11403.
17. **Feinstein, E., T. Druck, K. Kastury, H. Berissi, S. A. Goodart, J. Overhauser, A. Kimchi, and K. Huebner.** 1995. Assignment of DAP1 and DAPK—genes that positively mediate programmed cell death triggered by IFN-gamma—to chromosome regions 5p12.2 and 9q34.1, respectively. Genomics **29:**305–307.
18. **Feinstein, E., D. Wallach, M. Boldin, E. Varfolomeev, and A. Kimchi.** 1995. The death domain: a module shared by proteins with diverse cellular functions. Trends Biochem. Sci. **20:**342–344.
19. **Frederickson, R. M., K. S. Montine, and N. Sonenberg.** 1991. Phosphorylation of eukaryotic translation initiation factor 4E is increased in Src-transformed cell lines. Mol. Cell. Biol. **11:**2896–2900.
20. **Gabig, T. G., P. L. Mantel, R. Rosli, and C. D. Crean.** 1994. Requiem: a novel zinc finger gene essential for apoptosis in myeloid cells. J. Biol. Chem. **269:**29515–29519.
21. **Gan, W., and R. E. Rhoads.** 1996. Internal initiation of translation directed by the 5′-untranslated region of the mRNA for eIF4G, a factor involved in the picornavirus-induced switch from cap-dependent to internal initiation. J. Biol. Chem. **271:**623–626.
22. **Gossen, M., and H. Bujard.** 1992. Tight control of gene expression in mammalian cells by tetracycline-responsive promoters. Proc. Natl. Acad. Sci. USA **89:**5547–5551.
23. **Goyer, C., M. Altmann, H. S. Lee, A. Blanc, M. Deshmukh, J. L. Woolford, Jr., H. Trachsel, and N. Sonenberg.** 1993. *TIF4631* and *TIF4632*: two yeast genes encoding the high-molecular-weight subunits of the cap-binding protein complex (eukaryotic initiation factor 4F) contain an RNA recognition motif-like sequence and carry out an essential function. Mol. Cell. Biol. **13:**4860–4874.
24. **Grifo, J. A., S. M. Tahara, M. A. Morgan, A. J. Shatkin, and W. C. Merrick.** 1983. New initiation factor activity required for globin mRNA translation. J. Biol. Chem. **258:**5804–5810.
25. **Hiremath, L. S., N. R. Webb, and R. E. Rhoads.** 1985. Immunological detection of the messenger RNA cap-binding protein. J. Biol. Chem. **260:**7843–7849.
26. **Imataka, H., H. S. Olsen, and N. Sonenberg.** A new translational regulator that is homologous to eukaryotic translation initiation factor 4G. EMBO J., in press.
27. **Jackson, R. J., M. T. Howell, and A. Kaminski.** 1990. The novel mechanism of initiation of picornavirus RNA translation. Trends Biochem. Sci. **15:**477–483.
28. **Kimchi, A.** 1992. Cytokine triggered molecular pathways that control cell cycle arrest. J. Cell. Biochem. **50:**1–9.
29. **Kirchweger, R., E. Ziegler, B. J. Lamphear, D. Waters, H.-D. Liebig, W. Sommergruber, F. Sobrino, C. Hohenadl, D. Blaas, R. E. Rhoads, and T. Skern.** 1994. Foot-and-mouth disease virus leader proteinase: purification of the Lb form and determination of its cleavage site on eIF-4γ. J. Virol. **68:**5677–5684.
30. **Kissil, J. L., L. P. Deiss, M. Bayewitch, T. Raveh, G. Khaspekov, and A. Kimchi.** 1995. Isolation of DAP3, a novel mediator of interferon-gamma-induced cell death. J. Biol. Chem. **270:**27932–27936.
31. **Lamphear, B. J., R. Kirchweger, T. Skern, and R. E. Rhoads.** 1995. Mapping of functional domains in eukaryotic protein synthesis initiation factor 4G (eIF4G) with picornaviral proteases. Implications for cap-dependent and cap-independent translational initiation. J. Biol. Chem. **270:**21975–21983.
32. **Lamphear, B. J., R. Yan, F. Yang, D. Waters, H. D. Liebig, H. Klump, E. Kuechler, T. Skern, and R. E. Rhoads.** 1993. Mapping the cleavage site in protein synthesis initiation factor eIF-4 gamma of the 2A proteases from human coxsackievirus and rhinovirus. J. Biol. Chem. **268:**19200–19203.
33. **Lazaris-Karatzas, A., K. S. Montine, and N. Sonenberg.** 1990. Malignant transformation by a eukaryotic initiation factor subunit that binds to mRNA 5′ cap. Nature **345:**544–547.
34. **Lazaris-Karatzas, A., and N. Sonenberg.** 1992. The mRNA 5′ cap-binding protein, eIF-4E, cooperates with v-*myc* or E1A in the transformation of primary rodent fibroblasts. Mol. Cell. Biol. **12:**1234–1238.

34a. **Levy-Strumpf, N., and A. Kimchi.** Unpublished results.

35. **Lin, T. A., X. Kong, T. A. Haystead, A. Pause, G. Belsham, N. Sonenberg, and J. C. Lawrence, Jr.** 1994. PHAS-I as a link between mitogen-activated protein kinase and translation initiation. Science **266:**653–656.
36. **Macejak, D. G., and P. Sarnow.** 1991. Internal initiation of translation mediated by the 5′ leader of a cellular mRNA. Nature **353:**90–94.
37. **Mader, S., H. Lee, A. Pause, and N. Sonenberg.** 1995. The translation initiation factor eIF-4E binds to a common motif shared by the translation factor eIF-4γ and the translational repressors 4E-binding proteins. Mol. Cell. Biol. **15:**4990–4997.
38. **Manzella, J. M., W. Rychlik, R. E. Rhoads, J. W. Hershey, and P. J. Blackshear.** 1991. Insulin induction of ornithine decarboxylase. Importance of mRNA secondary structure and phosphorylation of eucaryotic initiation factors eIF-4B and eIF-4E. J. Biol. Chem. **266:**2383–2389.
39. **Merrick, W. C., and J. W. B. Hershey.** 1996. The pathway and mechanism of eukaryotic protein synthesis, p. 31–70. *In* J. W. B. Hershey, M. Mathews, and N. Sonenberg (ed.), Translational control. Cold Spring Harbor Laboratory Press, Cold Spring Harbor, N.Y.
40. **Meyuhas, O., D. Avni, and S. Shama.** 1996. Translational control of ribosomal protein mRNAs in eukaryotes, p. 363–388. *In* J. W. B. Hershey, M. Mathews, and N. Sonenberg (ed.), Translational control. Cold Spring Harbor Laboratory Press, Cold Spring Harbor, N.Y.
41. **Miura, M., R. M. Friedlander, and J. Yuan.** 1995. Tumor necrosis factor-induced apoptosis is mediated by a CrmA-sensitive cell death pathway. Proc. Natl. Acad. Sci. USA **92:**8318–8322.
42. **Morley, S. J.** 1994. Signal transduction mechanisms in the regulation of protein synthesis. Mol. Biol. Rep. **19:**221–231.
43. **Morley, S. J., and J. A. Traugh.** 1989. Phorbol esters stimulate phosphorylation of eukaryotic initiation factors 3, 4B, and 4F. J. Biol. Chem. **264:**2401–2404.
44. **Oh, S. K., M. P. Scott, and P. Sarnow.** 1992. Homeotic gene Antennapedia mRNA contains 5′-noncoding sequences that confer translational initiation by internal ribosome binding. Genes Dev. **6:**1643–1653.
45. **Ohlmann, T., M. Rau, V. M. Pain, and S. J. Morley.** 1996. The C-terminal domain of eukaryotic protein synthesis initiation factor (eIF)4G is sufficient to support cap-independent translation in the absence of eIF4E. EMBO J. **15:**1371–1382.
46. **Pause, A., G. J. Belsham, A. C. Gingras, O. Donze, T. A. Lin, J. C. Lawrence,**

Jr., and N. Sonenberg. 1994. Insulin-dependent stimulation of protein synthesis by phosphorylation of a regulator of 5′-cap function. Nature **371:**762–767.
47. **Rost, B., and C. Sander.** 1993. Prediction of protein secondary structure at better than 70% accuracy. J. Mol. Biol. **232:**584–599.
48. **Rost, B., and C. Sander.** 1994. Combining evolutionary information and neural networks to predict protein secondary structure. Proteins **19:**55–72.
49. **Sarnow, P.** 1989. Translation of glucose-regulated protein 78/immunoglobulin heavy-chain binding protein mRNA is increased in poliovirus-infected cells at a time when cap-dependent translation of cellular mRNAs is inhibited. Proc. Natl. Acad. Sci. USA **86:**5795–5799.
50. **Shantz, L. M., and A. E. Pegg.** 1994. Overproduction of ornithine decarboxylase caused by relief of translational repression is associated with neoplastic transformation. Cancer Res. **54:**2313–2316.
51. **Sonenberg, N.** 1996. mRNA 5′ cap-binding protein eIF4E and control of cell growth, p. 245–270. *In* J. W. B. Hershey, M. Mathews, and N. Sonenberg (ed.), Translational control. Cold Spring Harbor Laboratory Press, Cold Spring Harbor, N.Y.
52. **Sonenberg, N., M. A. Morgan, W. C. Merrick, and A. J. Shatkin.** 1978. A polypeptide in eukaryotic initiation factors that crosslinks specifically to the 5′-terminal cap in mRNA. Proc. Natl. Acad. Sci. USA **75:**4843–4847.
53. **Sonenberg, N., K. M. Rupprecht, S. M. Hecht, and A. J. Shatkin.** 1979. Eukaryotic mRNA cap binding protein: purification by affinity chromatography on Sepharose-coupled m^7GDP. Proc. Natl. Acad. Sci. USA **76:**4345–4349.
54. **Tahara, S. M., M. A. Morgan, and A. J. Shatkin.** 1981. Two forms of purified m7G-cap binding protein with different effects on capped mRNA translation in extracts of uninfected and poliovirus-infected HeLa cells. J. Biol. Chem. **256:**7691–7694.
55. **Tiefenbrun, N., D. Melamed, N. Levy, D. Resnitzky, I. Hoffmann, S. I. Reed, and A. Kimchi.** 1996. Alpha interferon suppresses the cyclin D3 and *cdc25A* genes, leading to a reversible G_0-like arrest. Mol. Cell. Biol. **16:**3934–3944.
56. **Vagner, S., M. C. Gensac, A. Maret, F. Bayard, F. Amalric, H. Prats, and A. C. Prats.** 1995. Alternative translation of human fibroblast growth factor 2 mRNA occurs by internal entry of ribosomes. Mol. Cell. Biol. **15:**35–44.
57. **Vito, P., E. Lacana, and L. D'Adamio.** 1996. Interfering with apoptosis: Ca(2+)-binding protein ALG-2 and Alzheimer's disease gene ALG-3. Science **271:**521–525.
58. **Yan, R., W. Rychlik, D. Etchison, and R. E. Rhoads.** 1992. Amino acid sequence of the human protein synthesis initiation factor eIF-4g. J. Biol. Chem. **267:**23226–23231.
59. **Zakeri, Z., D. Quaglino, T. Latham, K. Woo, and R. A. Lockshin.** 1996. Programmed cell death in the tobacco hornworm, Manduca sexta: alteration in protein synthesis. Microsc. Res. Tech. **34:**192–201.